Int. J. Electrochem. Sci., 16 **(2021)** Article ID: 210770, doi: 10.20964/2021.07.21

International Journal of
ELECTROCHEMICAL
SCIENCE
www.electrochemsci.org

The inhibition effect of eco-friendly sodium dodecyl sulfate on the corrosion behavior of SUS304L, SUS304H, and SUS316H stainless steels in sulfuric acid solution

Magdy A.M. Ibrahim[1,*], *Mossad M. Hamza*[1], *Jacek Ryl*[2,*], *Mohammed A. Amin*[3,*], *Sayed S. Abd El Rehim*[1]

[1] Faculty of Science, Chemistry Department, Ain Shams University, Cairo 11566, Egypt
[2] Institute of Nanotechnology and Materials Engineering, Faculty of Applied Physics and Mathematics, Gdansk University of Technology, Narutowicza 11/12, 80-233 Gdansk, Poland
[3] Department of chemistry, College of Science, Taif University, P.O. Box 11099, Taif 21944, Saudi Arabia
[*]E-mail: imagdy1963@hotmail.com

Received: 28 February 2021 / *Accepted:* 24 April 2021 / *Published:* 31 May 2021

The inhibition characteristics of an anionic surfactant, sodium dodecyl sulfate (SDS), against the corrosion of SUS304L, SUS304H, and SUS316H stainless steels in 0.5 M sulfuric acid were assessed utilizing Tafel extrapolation and electrochemical impedance spectroscopy (EIS) methods. The investigated surfactant behaved as a mixed-type inhibitor in all cases, as reported by the results of polarization measurements. For all stainless steel tested, the inhibition efficacy (η%) improved as the SDS concentration enhanced, attaining its maximum value at the SDS's critical micelle concentration (CMC). At a given C_{SDS}, in all cases, the η% values are found to decline with raising temperature referring to the physisorption of the inhibitors' molecules. The sulfuric acid corrosion of the three stainless steels tested was significantly reduced by the SDS molecules *via* adsorption following the Temkin adsorption isotherm. The stability and durability of such inhibitor molecules' adsorbed protective films were studied using EIS performed at various submerging periods (5-120 min). The outcomes of the polarization and impedance measurements are very similar. The various standard thermodynamic functions for the inhibitor molecules' adsorption process, namely ΔG^{o}_{ads}, ΔH^{o}_{a} and ΔS^{o}_{a} were estimated and discussed.

Keywords: Adsorption isotherm; Sodium dodecyl sulfate; Stainless steel; Tafel extrapolation method; EIS.

1. INTRODUCTION

Where a material that must withstand corrosive environments is needed, austenitic stainless steels are commonly used. It possesses excellent mechanical properties, the high amount of Ni and Cr in

austenitic stainless steels also produces exceptional corrosion resistance [1]. Furthermore, many austenitic stainless steels are weldable and formable. Grades SUS304 and SUS316 are typical examples of the more regularly applied class of austenitic stainless steel. The grade SUS316 contains the higher content of Mo which promotes this grade to possess increased corrosion resistance. The presence of a sound, unseeable, thin, robust, and the remarkably compact passive film explains stainless steel's high corrosion resistance [2]. The presence of an anion and the anode potential have been reported to stimulate the stability of passive films. Even though stainless steels exhibit a perfect resistance for corrosion in several offensive media, they tolerate corrosion in acid solutions [3-10]. One of the methods effectively manages the corrosion processes is the inclusion of corrosion inhibitors. General speaking published data concerning the corrosion inhibition of stainless- steel, in comparison with steel, are rare. Surfactants have recently been recognized as an important class of organic substances that are widely utilized as corrosion inhibitors[5, 11-19]. The surfactants act as corrosion inhibitors possesses low price and at the same time, it could be considered as an eco-friendly substance [14,20]. Sodium dodecyl sulfate (SDS) could be considered as one of the most important surfactants [14]. Surfactant molecules can adsorb on the solid surface under the right conditions, forming a systematized structure or membrane that can protect metals from corrosion in aggressive media. Surfactant hindrance properties are often defined as a concentration of surfactant, referred to as the critical micelle concentration "CMC." At the CMC, a surfactant can form micelles (ordered structures) that coexist with segregated molecules in an equilibrium determined by the hydrophobic reciprocation between the surfactant hydrocarbon rear ends and the water, as well as the engaging hydration and repulsive electrostatic forces on the hydrophilic heads.

The primary target of this sight is to look into the corrosion inhibitory characteristics of SDS as an anionic surfactant on austenitic stainless steels SUS304L, SUS304H, and SUS316H in 0.5 M H_2SO_4. Moreover, the adsorption isotherms were investigated to determine the adsorption process parameters to shed more light on the adsorption mode.

2. EXPERIMENTAL

ABD Modern Foundries Company, Egypt, produced the austenitic stainless-steel specimens utilized in this investigation. The working electrode (WE) was a stainless-steel alloy with a diameter of 5 mm, which was embedded in a glass tube coated with epoxy resin (0.28 cm^2). Table 7 lists the chemical components that make up these alloys. The WE are polished with a series of polishing pads, beginning with a coarse grade and working up to a fine grade, then washed thoroughly with purified water. The counter electrode was made of platinum wire. Potentials were evaluated with a SCE as a reference. A computer-assisted Potentiostat ACM is being used to allow the measurements in a classic cell. A water thermostat was used to keep the desired temperature for the cell ±1.0^{o}C. By sweeping the potential towards more noble potentials (scan rate 10 mVs^{-1}), the potentiodynamic (E/j) responses were traced.

EIS was tested at the OCP using an a.c. signal with a frequency range of 30 kHz to 1 Hz and an amplitude of 10 mV peak to peak. Triplicate runs were accomplished to guarantee that the findings were accurate. The equivalent circuit was tested using a software ACM Instrument-Gill AC automated

potentiostat ZRA EIS/AC Impedance Galvanostats and LPR meters, and using Nyquist and Bode graphs, the values of R_{ct} and C_{dl} for the current systems were calculated. The anionic surfactant tested, sodium dodecyl sulfate, SDS, $CH_3(CH_2)_{11}OSO_3Na$ has the chemical structure shown below:

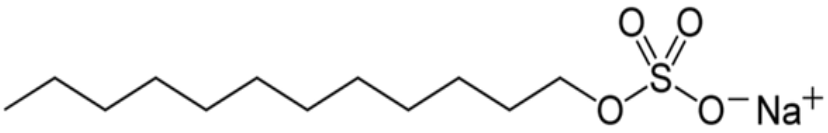

Scheme 1. Chemical structure of sodium dodecyl sulfate

3. RESULTS AND DISCUSSION

3.1. Potentiodynamic E/j curves

Figs.1-3 illustrate the impact of the inclusion of different SDS concentrations on the polarization behavior of SUS304L, SUS304H, and SUS316H. At 25°C, measurements were accomplished in 0.5 M H_2SO_4 solution. Table 1 explores the corrosion parameters, namely the corrosion potential, E_{corr}, and the corrosion current, j_{corr}, for the three alloys as a function of SDS concentration (C_{SDS}). Careful investigation of the data in Table 1, referred that the inclusion of low concentrations of SDS (10^{-3} M) enhances j_{corr} indicating an acceleration of the corrosion of alloy SUS304L in 0.5 M H_2SO_4 solution. However, the inclusion of higher concentrations of SDS (> 10^{-3} M) decreases j_{corr}, indicating inhibition of corrosion. In many cases, an acceleration of corrosion processes is reported in the literature particularly for cases involving low additive concentrations [5,21].

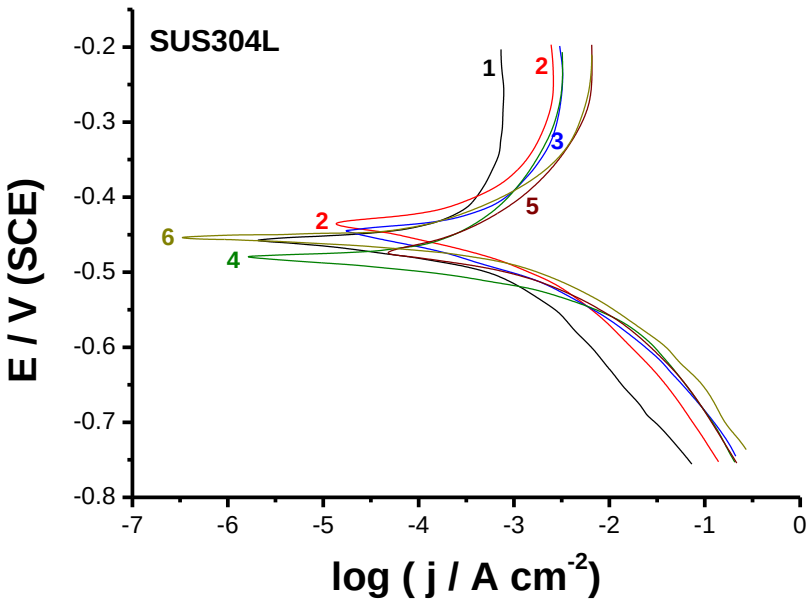

Figure 1. Polarization behavior measured for SUS304L alloy in 0.50 M sulfuric acid solutions devoid of and containing diverse concentrations of SDS at a potential sweep rate of 10 mV s^{-1} and 25° C. (1) Blank; (2) 10^{-3} M; (3) 10^{-2} M; (4) 0.02 M; (5) 0.03 M and (6) 0.04 M SDS.

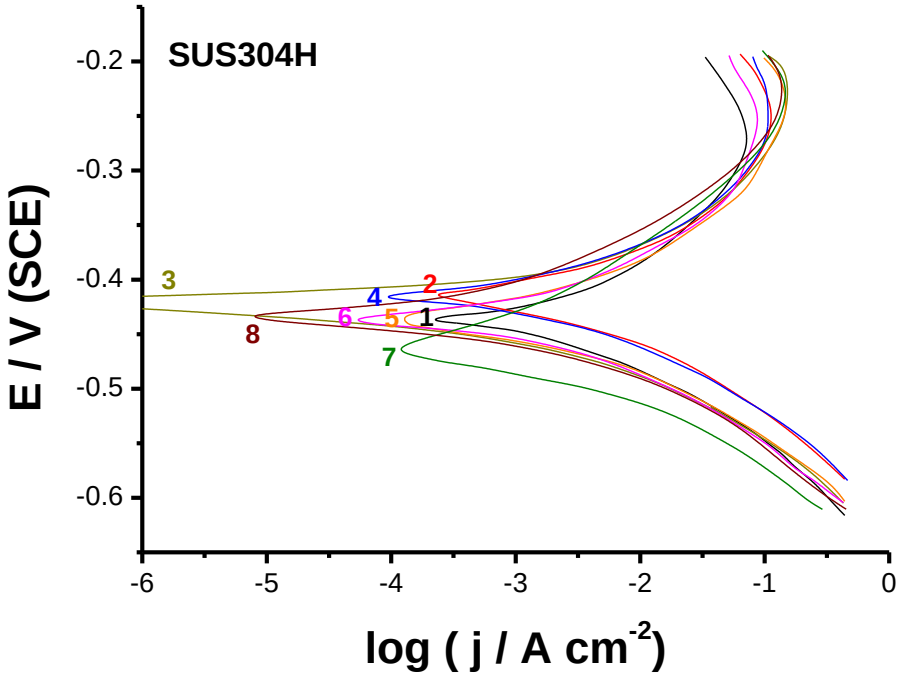

Figure 2. Polarization behavior measured for SUS304H alloy in 0.50 M sulfuric acid solutions devoid of and containing diverse concentrations of SDS at a potential sweep rate of 10 mV s^{-1} and 25º C. (1) Blank; (2) 10^{-5} M; (3) 10^{-4} M; (4) 10^{-3} M; (5) 10^{-2} M; (6) 0.02 M; (7) 0.03 M and (8) 0.04 M SDS.

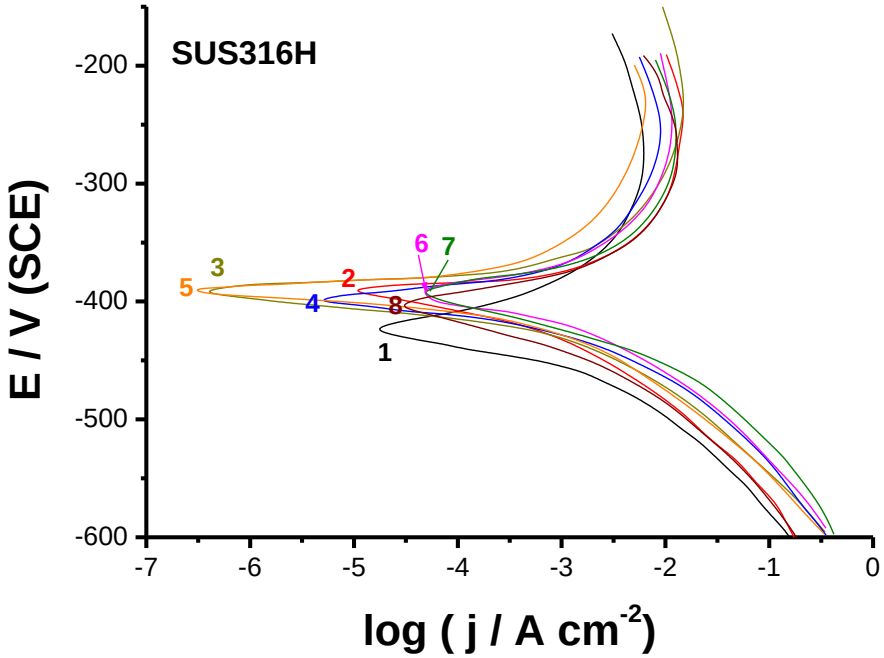

Figure 3. Polarization behavior measured for SUS316H alloy in 0.50 M sulfuric acid solutions devoid of and containing diverse concentrations of SDS at a potential sweep rate of 10 mV s^{-1} and 25º C. (1) Blank; (2) 10^{-6} M; (3) 10^{-5} M; (4) 10^{-4} M; (5) 10^{-3} M; (6) 10^{-2} M; (7) 0.02 M and (8) 0.03 M SDS.

In an earlier study, the rates of corrosion were raised when low concentrations of surfactants with long-chain alkyl groups existed in H_2SO_4 solutions [21]. The increased rate of corrosion may be due to a decrease in the overpotential associated with the H_2 evolution reaction. It may also be as a result of impurity particle adsorption on the alloy surface, which lowers the metal-binding energy and, as a result, influences the mechanism of the H_2 overpotential. The existence of concentration required for inhibition appears to be dependent on the additive's composition, the aggressive medium's concentration, the solution temperature, and the nature of corroding materials. For all tested alloys, the presence of all concentrations of SDS used is found to decrease the values of j_{corr} (Table 1) proportionally to C_{SDS}. The decrease in j_{corr} values is most readily attributed to SDS molecule adsorption and the subsequent formation of a protective membrane of SDS molecules on the alloy surface. This membrane blocks the active area available for the corrosion reaction and consequently, the corrosion rate is mitigated. On the other hand, the inclusion of various concentrations of SDS into the sulfuric acid solution has no significant effect on the values of E_{corr} suggesting SDS as a mixed-type inhibitor. The cathodic Tafel slope β_c (791 mV dec^{-1}) and the anodic Tafel slope β_a (707 mV dec^{-1}), on the other hand, remained nearly unchanged. The constancy of the Tafel slopes β_c and β_a indicate that the adsorbed SDS molecules stop up the energetic sites for corrosion reactions without affecting their mechanisms.

Table 1. Corrosion parameters derived from Figs. 1-3, together with η% values estimated for SUS304L, SUS304H, and SUS316H in 0.5 M sulfuric acid with and without SDS of diverse concentrations at 25° C.

[SDS] / M	SUS304L			[SDS] / M	SUS304H			[SDS] / M	SUS316H		
	$-E_{corr}$ (mV)	J_{corr} ($mAcm^{-2}$)	η%		$-E_{corr}$ (mV)	J_{corr} ($mAcm^2$)	η%		$-E_{corr}$ (mV)	J_{corr} (mA cm^{-2})	η%
0.0	460	22.3	-	0	420	53.5	18.7	0	427	65.4	-
10^{-3}	452	23.7	-	10^{-5}	425	43.5	22.2	10^{-6}	410	29.8	54.5
10^{-2}	457	19.3	13.2	10^{-4}	422	41.6	31.8	10^{-5}	395	29.1	55.5
0.02	473	16.7	25.2	10^{-3}	424	36.5	54.2	10^{-4}	415	21.0	67.8
0.03	475	15.9	28.8	10^{-2}	418	24.5	65.7	10^{-3}	398	15.0	77.1
0.04	465	14.2	36.2	0.02	440	18.4	64.7	10^{-2}	392	17.6	73.1
				0.03	445	16.1	65.0	0.02	393	15.9	75.8
				0.04	418	17.8		0.03	404	12.7	80.5

Equation (1) is used to calculate the inhibition efficiency (η%) for each studied alloy as a function of C_{SDS}, Table 2.

$$\eta\% = 100\left(1 - \frac{j_{corr}}{j^0_{corr}}\right) \quad (1)$$

For each alloy, higher efficiency is evident at C_{SDS} values close to the CMC, this entails the formation of a bimolecular layer on the electrode/solution interface [19] or the formation of a large molecule, i.e. a micelle, at a higher concentration. The CMC of SDS is reported in the literature as 2.5 x 10^{-3} M, at 25ºC [5].

The impact of temperature (10-75°C) on the polarization behavior of SUS304L, SUS304H, and SUS316H alloys in 0.5M H_2SO_4 solution devoid of and containing 0.02M SDS was carried out and the obtained corrosion parameters are collected in Table 2. The magnitude of η% was also computed for the three studied alloys at each temperature using Eq. (1), Table 2.

Table 2. Corrosion parameters and η% values deduced from polarization measurements for alloys SUS304L, SUS304H, and 304SUS316H in 0.5M H_2SO_4 solution devoid of and containing 0.02M SDS at different temperatures.

T/ °C	SUS304L				SUS304H				SUS316H			
	0.5M sulfuric acid	0.5M sulfuric acid + 0.02 M SDS			0.5M sulfuric acid	0.5M sulfuric acid + 0.02 M SDS			0.5M sulfuric acid	0.5M sulfuric acid + 0.02 M SDS		
	j_{corr} ($mAcm^{-2}$)	j_{corr} ($mAcm^{-2}$)	$-E_{corr}$ (mV)	η %	j_{corr} ($mAcm^{-2}$)	j_{corr} ($mA\ cm^{-2}$)	$-E_{corr}$ (mV)	η %	j_{corr} ($mAcm^{-2}$)	j_{corr} ($mAcm^{-2}$)	$-E_{corr}$ (mV)	η %
10	18.21	12.72	480	30.2	45.85	15.11	485	67.0	47.75	8.97	372	81.2
25	22.28	16.66	460	25.2	53.52	18.38	440	65.7	65.63	15.85	393	75.8
35	22.30	18.25	418	18.3	64.28	22.18	427	65.5	76.50	18.90	372	75.3
45	22.64	18.70	409	17.4	65.00	22.88	410	64.8	78.10	20.14	360	74.2
55	24.57	20.40	388	17.0	67.00	24.82	409	63.0	80.58	20.94	350	74.0
65	32.00	26.75	380	16.4	70.88	30.34	378	57.2	112.5	31.28	337	72.2
75	34.13	28.80	372	15.6	71.16	32.49	371	54.3	113.9	33.30	340	70.8

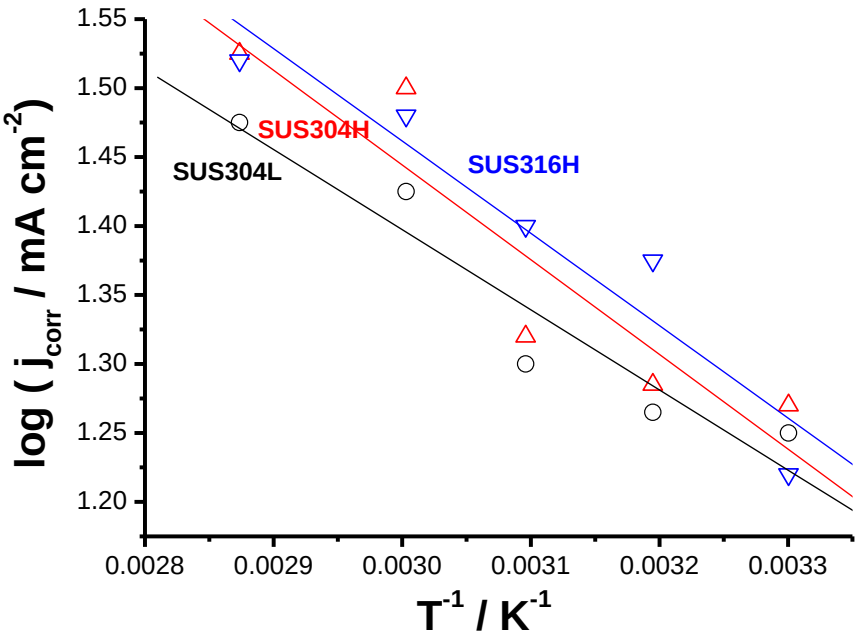

Figure 4. Arrhenius plots for SUS304L, SUS304H, and SUS316H alloys in 0.02 M SDS-containing sulfuric acid solution (0.50 M).

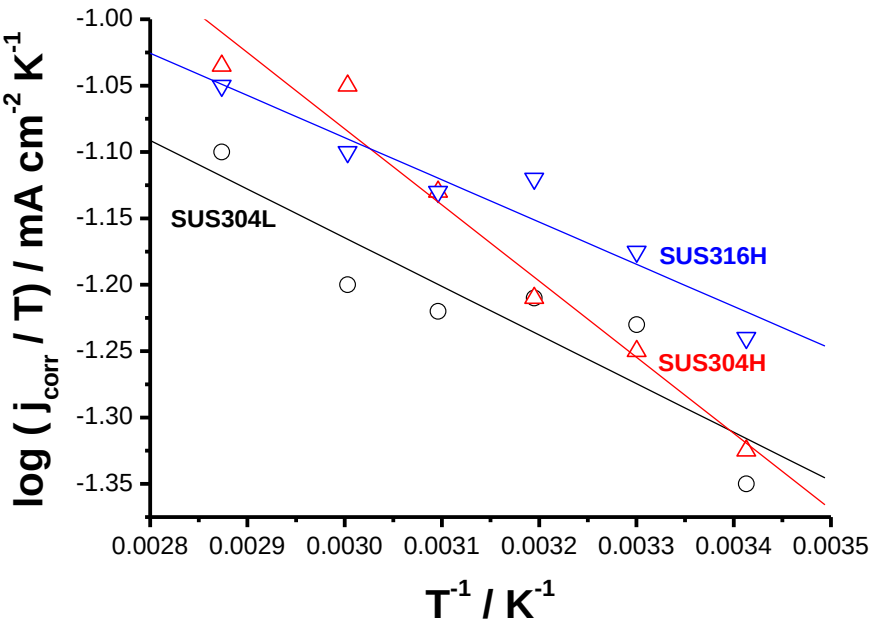

Figure 5. Transition state plots for SUS304L, SUS304H, and SUS316H alloys in 0.02 M SDS-containing sulfuric acid solution (0.50 M).

It follows from Table 2 that, in all cases, increasing the solution temperature increases j_{corr} (i.e., enhanced corrosion rate), corresponding to decreased η% value. These findings refer to the physisorption characteristics of SDS molecules. Representing the relation between log j_{corr} and 1/T (Arrhenius plot) for the three alloys in 0.5 M sulfuric acid involving 0.02 M SDS produce straight lines as manifested in Fig. 4. The apparent activation energy values, E^o_a computed from the slopes of these lines for the blank solutions were 8.8, 6.8, and 11.0 kJ mol^{-1} for SUS304L, SUS304H, and SUS316H alloys, respectively. However, the magnitudes of E^o_a obtained for the inhibited solutions (0.02 M SDS) were 10.4, 9.96, and 13.6 kJ mol^{-1} for SUS304L, SUS304H, and SUS316H alloys, respectively.

The E^o_a values acquired from the blank solution are lower than those acquired from the inhibited solution, indicating that the presence of SDS in sulfuric acid raises the energy barrier for corrosion reactions. These findings suggest that the presence of SDS causes the corrosion reaction to be pushed to the higher activation energy surface sites. The comparison of corrosion activation energies in the absence and existence of SDS molecules, as well as the temperature dependence of inhibition performance, reveal important details about the inhibitor adsorption mechanism. The creation of a physically adsorbed layer of the SDS molecules is confirmed by the decline in the efficiency of inhibition value when the temperature is raised. The enhancement in E^o_a in the existence of inhibitor relative to its absence when the temperature is elevated also supports the SDS molecules' physical adsorption.

The enthalpy of activation, ΔH^o_a, and entropy of activation, ΔS^o_a of the corrosion process was calculated by applying equation (2):

$$\text{Rate} = RT / Nh \exp(\Delta S^o_a / R) \exp(-\Delta H^o_a / RT) \quad (2)$$

where N is Avogadro's number, h is Blank's constant. Plotting of log (j_{corr}/T) versus 1/T yielded a straight line with a slope of ($-\Delta H^o_a$ / 2.303R) and an intercept of (log R/Nh- ΔS^o_a 2.303R), Fig. 5. The

computed values of ΔH^o_a and ΔS^o_a are provided in Table 3. The positive value of ΔH^o_a means an endothermic response to the adsorption. On the steel surface, the inhibitor has formed a stable layer because the values of E^o_a are larger than those of ΔH^o_a [22]. SDS is a good corrosion inhibitor, according to the results. In the absence and existence of SDS, the activation entropy ΔS^o_a is high and negative, meaning that: in the rate-determining step, the activated complex is treated as an interaction rather than a dissociation step, and disordering decreases as the reaction progresses from reactants to the activated complex [23].

Table 3. Thermodynamic activation functions (ΔH^o_a and ΔS^o_a) recorded for the corrosion of SUS304L, SUS304H, and SUS316H alloys in 0.5M H_2SO_4 and in (0.5M sulfuric acid and 0.02M SDS) solutions estimated by using transition state equation.

SUS304L (0.09Mo)				SUS304H (1.15 Mo)				SUS316H (2.0 Mo)			
ΔH^o_a (kJ/mol)		$-\Delta S^o_a$ (J/mol K)		ΔH^o_a (kJ/mol)		$-\Delta S^o_a$ (J/mol K)		ΔH^o_a (kJ/mol)		$-\Delta S^o_a$ (J/mol K)	
0.5M sulfuric acid	0.5M H_2SO_4 + 0.02M SDS	0.5M H_2SO_4	0.5M H_2SO_4 + 0.02M SDS	0.5M H_2SO_4	0.5M H_2SO_4 + 0.02M SDS	0.5M H_2SO_4	0.5M H_2SO_4 + 0.02M SDS	0.5M H_2SO_4	0.5M H_2SO_4 + 0.02M SDS	0.5M H_2SO_4	0.5M H_2SO_4 + 0.02M SDS
6.14	8.0	246	242	4.35	7.42	244	243	9.27	13.83	226	223

3.2. Electrochemical impedance measurements

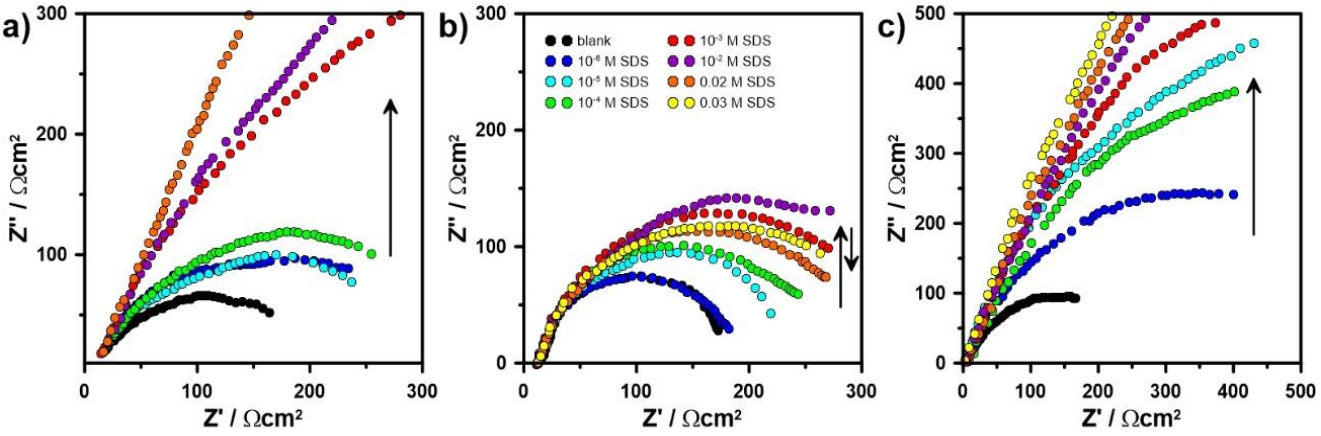

Figure 6. Complex-plane impedance diagrams recorded for (a) SUS304L, (b) SUS304H, and (c) SUS316H in 0.50 M sulfuric acid in the absence and existence of various SDS concentrations at the particular E_{corr} values.

Next, the electrochemical impedance spectroscopy (EIS) responses were conducted at the OCP in order to cross-verify previously presented values of SDS inhibition efficiency towards each studied stainless steel, i.e. SUS304L, SUS304H, and SUS316H. These experiments were accomplished in 0.5 M H_2SO_4 solution at 25°C for various SDS concentrations between 10^{-6} and $3*10^{-2}$ M. The Nyquist plots of the obtained impedance spectra are summarized in Figs. 6a-c.

Based on the impedance spectra shape, it is evident the corrosion reaction is under charge transfer control [24]. For each studied stainless steel, the diameter of the semicircle enhances with SDS concentration enhance, which is evidence of the successful corrosion inhibition mechanism. This tendency may outcome from the fact that as the inhibitor concentration rises, so does adsorption and surface coverage; hence, the surface is successfuly isolated from the medium [25].

A simple electric equivalent circuit (EEC), consisted of series resistance (solution resistance) in sequence with a charge-transfer resistance R_{CT} and a capacitive part C in parallel, was chosen for the fitting procedure. A numerical analysis of the impedance spectra, in all cases studied, has exhibited the semicircles drawn by the impedance spectra in the Nyquist projection to be flattened. This behavior should be explained by the coexistence of the double-layer capacitance, passive film capacitance and SDS layer capacitance, all represented by the time constants of similar kinetics and producing frequency dispersion of capacitance. A constant phase element (CPE) is frequently utilized to characterize the parallel quasi-capacitance of heterogeneous surfaces [26]. To estimate the effective parallel capacitance C_{EFF}, based on the CPE, an approximation for normal distribution of frequency dispersion of capacitance was used [27]. The impedance parameters R_{CT} and C_{EFF} generated from the impedance spectra are shown in Table 4.

The shape of impedance spectra depends on the concentration of SDS and the composition of stainless steel. The behavior of each investigated steel in absence of the studied corrosion inhibitor is similar, however, expectedly SUS316H is characterized by slightly higher corrosion resistance towards sulfuric acid, with charge transfer resistance being approximately 40% higher compared to SUS304L and SUS304H steels.

The R_{CT} values at any inhibitor concentration and for each alloy may be employed to evaluate the η% utilizing the following formula:

$$\eta\% = (1 - R_{CT} / R^0_{CT}) \times 100 \quad (5)$$

where R^0_{CT} and R_{CT} are the charge-transfer resistances for corrosive media containing and free from inhibitors, respectively. The determined η% are included in Table 4. In all cases, the η% enhances with increasing the SDS concentration. Comparing the values of η% for the three alloys, it is found that the values of η% decrease in the order: SUS316H > SUS304L > SUS304H. These data are on the same track as those acquired from potentiodynamic polarization measurements and proceed in the same direction. The inhibition effect is particularly strong for SUS316H, where the inclusion of even 10^{-6} M SDS causes corrosion inhibition exceeding 60%.

Furthermore, when analyzing the quasi-capacitive changes, one can observe that C_{EFF} is diminished with R_{CT} increase, as the corrosion inhibition effect is enhanced. The adsorption and production of a barrier thin layer of SDS molecules at the alloy surface is responsible for these effects [24].

Table 4. AC Impedance data (R_{ct} and C_{dl}) and η% recorded for SUS304L, SUS304H, and SUS316H alloys in 0.50 M H_2SO_4 solution devoid of and containing diverse SDS concentrations, at 25°C.

[SDS] / M	SUS304L			[SDS] / M	SUS304H			[SDS] / M	SUS316H		
	R_{CT} (Ω cm^2)	C_{EFF} (μF cm^{-2})	η %		R_{CT} (Ω cm^2)	C_{EFF} (μF cm^{-2})	η %		R_{CT} (Ω cm^2)	C_{EFF} (μF cm^{-2})	η %
blank	193.3	172.6	-	0.00	173.8	266.0	-	0.00	266.7	676.3	-
10^{-6}	270.7	415.5	28.85	10^{-6}	197.0	238.0	11.7	10^{-6}	711.7	200.8	62.5
10^{-5}	247.2	374.6	22.2	10^{-5}	241.2	237.3	27.9	10^{-5}	1049.3	195.6	74.7
10^{-4}	321.6	367.8	40.2	10^{-4}	275.9	227.5	37.0	10^{-4}	1266.0	185.6	78.9
10^{-3}	1266.3	357.0	84.8	10^{-3}	362.5	225.0	52.03	10^{-3}	1292.0	165.0	79.4
10^{-2}	1530.0	351.9	87.4	10^{-2}	392.0	234.0	55.7	10^{-2}	1995.0	175.0	86.6
0.02	1600.0	345.0	88.0	0.02	420.0	220.0	58.3	0.02	2200.0	170.0	87.9
0.03	1630.0	337.0	88.2	0.03	455.0	226.5	61.8	0.03	2352.0	159.0	88.7

The plausible explanation of the exceptional SDS inhibition efficiency towards SUS316H steel is connected with the Mo species existing in the passive film. These are principally ionic compounds, present within the passive film. Under strongly acidic conditions Mo tends to precipitate as MoO_3 oxides, according to Pourbaix diagrams [28]. The forming of an insoluble MoO_3 and a protective oxide film, which slows the corrosion process, is thought to be responsible for the improved corrosion resistance of stainless steels in sulfuric acid. Moreover, it is reported that Mo is useful to enhance re-passivation characteristics by decreasing the number of point defects in the film [22].

Immersion time investigations were performed using AC impedance in 0.50 M H_2SO_4 and 0.02M SDS at the respective OCP and 25ºC for the SUS304L, SUS304H, and SUS316H alloys respectively (the results are not included here). However, the impedance parameters R_{ct} and C_{dl} deduced from these data are tabulated in Table 6. In general, it is noticed that R_{ct} enhances at first and then tends to diminish with increasing the submerging time. The rise in the values of R_{ct} is assigned to the substitute of H_2O molecules and acid anions from the surface of the alloy by adsorbed SDS molecules [29]. It seems that such a process takes place relatively fast. However, the decrease in R_{ct} values can be interpreted in terms of the increase of the cohesive forces among the SDS adsorbed molecules on the surface of the alloy [30].

The charge of the metal surface, the surfactant's dipole moment charge, and the adsorption of other ionic species all play a role in surfactant adsorption on corroding metals, if the adsorption is electrostatic [31]. In the electrostatic adsorption process, the potential of zero charge (PZC), usually determined from impedance measurements conducted at various overpotentials[32], is crucial [27]. The

complex-plane impedance plots for alloy SUS316H in 0.5M sulfuric acid solution were recorded at different potentials (ranged between -700 to -300 mV_{SCE}). The relationship between C_{dl} derived from Nyquist plots versus each applied potential is discussed in Fig.7, which is a parabolic curve characterized by a minimum capacitance of approximately -450 mV.

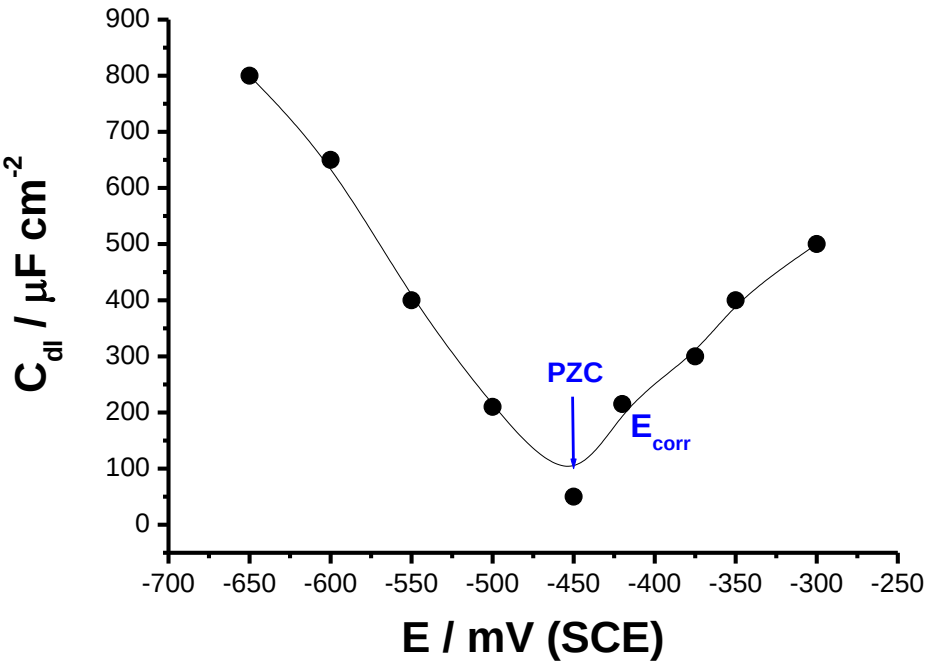

Figure 7. The relationship between C_{dl} and the applied potential E for SUS304H alloy in 0.50 M sulfuric acid solution at 25° C.

This value is more negative than E_{corr} of the alloy in 0.5M H_2SO_4 indicating that the alloy surface is positively charged at E_{corr}. Therefore, one can conclude that upon the insertion of SDS to the acid solution, immediately, the negatively charged head of the inhibitor is physically adsorbed on the stainless steel surface by electrostatic attraction force, while the hydrophobic ($C_{12}H_{25}$-) long tail forced the liquid medium to set on the alloy surface [30]. The adsorbed inhibitor covered a large area of the alloy surface and involved inhibition. As the immersion time increased, many inhibitor anions were adsorbed on the surface, leading to the increase in repression performance. Later, the inhibition anions' adsorption density rises to the point where coherent forces of interaction between the long tail ($C_{12}H_{25}$-) occur. At this stage, many of the hydrocarbon chains adsorbed anions were expected to go away from the surface and aggregate to form hemimicelles. This will lead to a decline in the effective area occupied by $C_{12}H_{25}^-$, SO_4^{2-} anions to a certain degree. In this way, we can understand why the η% of SDS diminished with a further long time of submerging.

3.3. Adsorption isotherm

The adsorption activity of the measured SDS was investigated using a variety of adsorption isotherms. Using data derived from the polarization and impedance measurements, the Temkin adsorption isotherm, Eq. (6), was discovered to be the most successful match for the adsorption behavior of SDS at the stainless-steel/solution interface, see Fig. 8.

$$a\,\theta = \ln (K_{ads}\, C) \qquad (6)$$

where θ is the extent of SDS molecule covering on the surface (θ = η /100), a is a molecular interaction parameter that is affected by the lateral interaction force between adsorbed inhibitor molecules on the surface as well as the extent of diversity in the stainless-steel specimen., C refers to the SDS concentration in the solution (C_{SDS}), and K_{ads} is the equilibrium constant for the inhibitor adsorption.

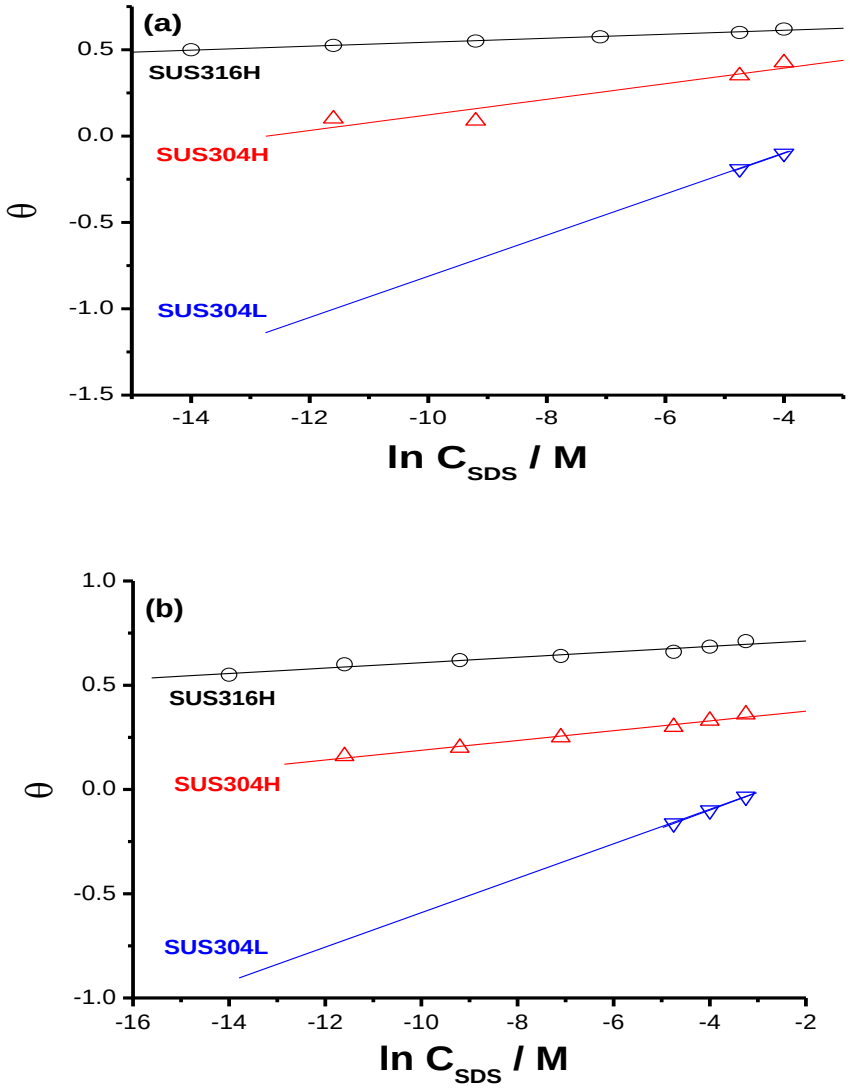

Figure 8. Curve matching of the polarization (a) and impedance (b) data acquired for SUS304L, SUS304H, and SUS316H alloys in 0.50 M sulfuric acid solution containing different SDS concentrations at 25° C, to Temkin adsorption isotherm.

Table 6 explores the values of K_{ads}, ΔG^o_{ads} and *a* for the three alloys. Equation (7) connects the equilibrium constant K_{ads} to the free energy of adsorption, ΔG^o_{ads} [33]:

$$\Delta G^o_{ads} = - RT \ln (55.5\, K_{ads}) \quad (7)$$

where R is the universal gas constant, T is the absolute temperature and the numerical value 55.5 represents the water concentration in the solution presented in mol L^{-1}. The data produced from E/j curves and EIS techniques are consistent. The positive value of a points out that the adsorbed molecules are are attracted to each other. The higher the magnitude of a, the more attraction force between the adsorbed molecules [34]. It has previously been demonstrated that the higher the value of K_{ads}, the easier the inhibitor adsorbs on the metal surface[35], implying that the inhibitor has stronger inhibition characteristics. The value of K_{ads}, which is the determining factor for the inhibition efficiency [36], for the three alloys, decreases in the order of SUS316H > SUS304H > SUS304L, indicating that the adsorption tendency of SDS decreases in the same order. The high negative numbers of ΔG^o_{ads} indicate that the adsorption of the SDS molecules is occurring spontaneously and with high efficiency. Accordingly, the results in Table 6 display that the values of ΔG^o_{ads} in the case of the three tested alloys decrease in the order: SUS316H > SUS304H > SUS304L.

Table 5. The impedance fitting parameters recorded for alloys SUS304L, SUS304H and 304SUS316H in 0.5M H_2SO_4 solution without and with 0.02M SDS at the corrosion potential focused on the duration of immersion at 25ºC.

Immersion time / min.	SUS304L		SUS304H		SUS316H	
	R_{ct} (Ω cm^2)	C_{dl} (μF cm^{-2})	R_{ct} (Ω cm^2)	C_{dl} (μF cm^{-2})	R_{ct} (Ω cm^2)	C_{dl} (μF cm^{-2})
0.0	600	345	530	220	1200	170
5	695	335	580	212	1080	185
10	956	320	570	215	1174	182
15	745	324	600	210	949	191
30	1159	315	650	198	1098	184
60	758	327	630	205	945	192
120	1200	310	620	204	890	189

Table 6. The binding constant of the inhibitor (K_{ads}), binding free energy (ΔG^o_{ads}) and molecular interaction parameter (*a*) estimated for SUS304L, SUS304H, and SUS316H in 0.5 M sulfuric acid solution containing various SDS concentrations at 25°C deduced by utilizing Temkin adsorption isotherm on the polarization and impedance result.

Alloy	**K_{ads}**		**ΔG^o_{ads} (kJ/mol)**		***A***	
	Polarization	Impedance	Polarization	Impedance	Polarization	Impedance
SUS304L	234	440	-23.5	- 25.0	6.35	8.30
SUS304H	823681	932880	- 43.7	-44.0	15.40	15.87
SUS316H	4.3×10^{15}	4.38×10^{17}	- 99.1	- 110.6	41.00	46.3

4. CONCLUSION

SDS behavious effectively as a good corrosion inhibitor for the SUS304L, SUS304H, and SUS316H alloys in 0.5M sulfuric acid as computed from the impedance and E/j responses. The η% enhances with enhancing the concentration of SDS and declines with raising the temperature. The studied SDS works as a mixed-type inhibitor. The adsorption of the studied SDS on stainless steel surfaces obeys Temkin adsorption isotherm and involves a physical adsorption mechanism. The thermodynamic parameters of SDS adsorption are computed from their adsorption isotherm. Comparing η% values for the three alloys, it is found that the magnitudes of η% decline in the order: SUS316H > SUS304L > SUS304H. This means that the more the Mo content in the alloy, the higher the resistance of the alloy towards the corrosion and consequently, the higher the η% in the presence of SDS.

ACKNOWLEDGEMENTS
The authors are also grateful to the Taif University Researchers Supporting Project number (TURSP-2020/03), Taif University, Taif, KSA.

References

1. C. J. Novak, *Handbook of Stainless Steels,* (1997), McGraw-Hill New York.
2. J. Sedriks, *Corrosion of Stainless Steels* (1996) 2nd ed John Willey & Sons Inc New York.
3. B. Jegdic, D.M. Drazic, and J. P. Popic, *J. Serb. Chem. Soc.*, 71(5) (2006)543.
4. I. Iliyasu, D. S. Yawas, and S. Y. Aku, *Adv Appl Sci Res,* 3(6) (2012) 3909
5. M. M. Hamza, S. S. Abd El Rehim, and M. A. M. Ibrahim, *Arab. J. Chem.*, 6 (2013) 413.
6. R. T. Loto, (2018) PLOS ONE https://doi.org/10.1371/journal.
7. M. P. Asfia, M. Rezaei, and G. Bahlakeh, *J. Mol. Liq.,* 315 (2020)113679.
8. Z. Shirazi, A. N. Golikand, and M. H. Keshavarz, *Composites Communications*, 22 (2020)100467.
9. A. A. Ayoola, O. S. I. Fayomi, I. G. Akande, O. A. Ayeni, O. Agboola, O. R. Obanla, O. G. Abatan, and C. J. Chukwuka, *J. Bio- and Tribo-Corrosion,* 6 (2020) 67.
10. A. A. Hermas, A. M. Elnady, and R. M. Ali, *Anti-Corrosion Methods and Materials*, https://doi.org/10.1108/ACMM-10-2018-2016.
11. R. D'Souza, T. P. Nithin, and N. Sirisha, *Int. J. Adv. Res. Sci. Eng.,* 4(2) (2015) 69.
12. A. Yousefi, and S. Javadian, *Int. J. Env. Sci.,* 5 (1) (2014) 99.
13. I. Aiad, S. M. Shaban, A. H. Elged and O.H. Aljoboury, (2018) *Egyptian Journal of Petroleum,* https://doi.org/10.1016/j.ejpe.2018.01.003.
14. M. A. Malik, M. A. Hashim, F. Nabi, S. A. AL-Thabaiti and Z. Khan, *Int. J. Electrochem. Sci.*, 6 (2011) 1927.
15. M. A. Migahed, E. M. S. Azzam, and A. M. Al-Sabagh, *Mat. Chem. Phys.*, 85 (2014) 273.
16. M. A. Migahed, and A. M. Al-Sabagh, *Chem. Eng. Comm.*,196 (9) (2009) 1054.
17. F. El-Taib Heakal, M. A. Deyab, M. M. Osman, M.I. Nessim, and A. E. Elkholy AE, *RSC Adv.*, 7 (2017) 47335.
18. J. Du, Q. Chen, Q. Liu, and X. Hu, (2018), *Inter. J. Corros.,* https://doi.org/10.1155/2018/9890504.
19. A. Fawzy, I.A. Zaafarany, H. A. Ali, and M. Abdallah, *Int. J. Electrochem. Sci.*, 13 (2018) 4575.
20. R. Aslam, M. Mobin, J. Aslam, H. Lgaz, I.-Min Chung, and S. Zehra, *J. Mol. Liq.,* 1228 (2021) 129751.
21. M. A. M. Ibrahim,, S. S. Abd El Rehim, and M. M. Hamza, Phys. Sci. Inter. J., 4(7) (2014) 940**.**
22. C. A. Schiller, and W. Strunz, *Electrochim Acta,* 46 (2001) 3619.

23. F. Bentiss, M. Traisnel, and M. Lagrenee, *J. Appl. Electrochem.*, 31(2001) 41.
24. Z. S.-Smialowska (1991) "*Electrochemical and optical Techniques for study of metallic corrosion*" Kluwer.
25. T. Zhao, and G. Mu, *Corros. Sci.*, 41 (1999) 1937.
26. X. Wu, H. Ma, S. Chen, Z. Xu, and A. Sui, *J. Electrochm. Soc.*, 146 (1999) 1847,
27. B. Hirschorn, M. E. Orazem, B. Tribollet, V. Vivier, and I. Frateur, *Electrochim Acta***,** 55 **(**2010**)** 6218**.**
28. A. Pardo, M. C. Merino, A. E. Coy, F. Viejo, R. Arrabal, and E. Matykina, *Corros. Sci.*, 50 (2008) 780.
29. H. Heon-Young, H. T.-Ho, L. J.-Hwan Bae, and D. W. Chun, *metals*, 8 (2018) 653.
30. S. Muralidharan, K. L. N. Phani, S. Pitchumani, S. Ravichandran, and S. V. K. Iyer, *J. Electrochem. Soc.*, 142 (1995) 1478.
31. Z. Abd El Hamid, T. Y. Sorror, H. A. El Dahan, and A. M. A. Omar, *Anti-Corrosion Methods and Material,* 45 (1998) 306.
32. H. Luo, Y.C. Guan, and K. N. Han, *Corros,* 54 (1998) 619.
33. M. A. Amin, *J. Appl. Electrochem.,* 36 (2006) 215.
34. Z. Szklarska, A. Smialowska, and G. Wieczorek, *Corros Sci,* 11(1971) 853.
35. A. M. Al-Mayouf. A. K. Al-Ameery, and A. A. Al-Suhybani, *Br. Corros. J.*, 36 (2001)128.
36. B. I. Obot, E. E. Ebenso, and M. M. Kabanda, *J. Environ. Chem. Eng.*, 1 (2013) 431.